

Learning Intelligent for Effective Sonography (LIFES) Model for Rapid Diagnosis of Heart Failure in Echocardiography

Lies Dina Liastuti^{1,2*}, Bambang Budi Siswanto¹, Renan Sukmawan¹,
Wisnu Jatmiko³, Idrus Alwi⁴, Budi Wiweko⁴, Aria Kekalih⁴,
Yosilia Nursakina^{4,5}, Rindayu Yusticia Indira Putri¹, Grafika Jati³,
Mgs M Luthfi Ramadhan³, Ericko Govardi¹, Aqsha Azhary Nur⁶

¹ Department of Cardiology and Vascular Medicine, Faculty of Medicine Universitas Indonesia, National Cardiovascular Center Harapan Kita Hospital, Jakarta, Indonesia

² Dr. Cipto Mangunkusumo Hospital, Jakarta, Indonesia

³ Faculty of Computer Science Universitas Indonesia, Indonesia

⁴ Faculty of Medicine, Universitas Indonesia, Jakarta, Indonesia

⁵ School of Public Health, Imperial College London, United Kingdom

⁶ The Johns Hopkins Bloomberg School of Public Health, Baltimore, United States

***Corresponding Author:**

Lies Dina Liastuti, MD. Dr. Cipto Mangunkusumo National Central Public Hospital. Jl. Pangeran Diponegoro No. 71, Jakarta 10430, Indonesia. Email: dr.liesdina@gmail.com.

†These authors contributed equally.

ABSTRACT

Background: The accuracy of an artificial intelligence model based on echocardiography video data in the diagnosis of heart failure (HF) called LIFES (Learning Intelligent for Effective Sonography) was investigated. **Methods:** A cross-sectional diagnostic test was conducted using consecutive sampling of HF and normal patients' echocardiography data. The gold-standard comparison was HF diagnosis established by expert cardiologists based on clinical data and echocardiography. After pre-processing, the AI model is built based on Long-Short Term Memory (LSTM) using independent variable estimation and video classification techniques. The model will classify the echocardiography video data into normal and heart failure category. Statistical analysis was carried out to calculate the value of accuracy, area under the curve (AUC), sensitivity, specificity, positive predictive value (PPV), negative predictive value (NPV), and likelihood ratio (LR). **Results:** A total of 138 patients with HF admitted to Harapan Kita National Heart Center from January 2020 to October 2021 were selected as research subjects. The first scenario yielded decent diagnostic performance for distinguishing between heart failure and normal patients. In this model, the overall diagnostic accuracy of A2C, A4C, PLAX-view were 92,96%, 90,62% and 88,28%, respectively. The automated ML-derived approach had the best overall performance using the 2AC view, with a misclassification rate of only 7,04%. **Conclusion:** The LIFES model was feasible, accurate, and quick in distinguishing between heart failure and normal patients through series of echocardiography images.

Keywords: Artificial intelligence, machine learning, echocardiography, heart failure.

INTRODUCTION

Cardiovascular disease remains the leading cause of death globally.¹ Current guidelines for diagnosing heart failure can only detect symptomatic and end-stage heart failure patients, who comprise only 12.2% of the population. However, heart failure patients who are asymptomatic or have a high risk of developing heart failure occupy 56% of the population and generally go undetected; hence affecting the prognosis of these patients.²

On the other hand, numerous studies have shown that artificial intelligence (AI) models have decent diagnostic quality in assisting the work of cardiologists, including diagnosing heart failure based on ECG and echocardiographic data.³⁻⁵ AI has proven to help with an accurate diagnosis, clinical management, and patient care.⁶ AI in cardiovascular imaging can also reduce costs, avoid missed diagnoses, false-positive diagnoses, inter-observer variability, and improve time efficiency.⁷ However, no studies have yet built AI algorithms to diagnose heart failure patients based on echocardiography videos. Specifically, no studies have optimized the use of many echocardiography views (e.g., long axis, 4-chamber view, and 2-chamber view) nor provided automatic measurement of EF and E/A ratio.

Thus, this study proposes an artificial intelligence model called LIFES (Learning Intelligent for Effective Sonography) developed in this study. It is the first study of artificial intelligence in the field of echocardiography in Indonesia that can quickly, precisely, and cost-efficiently distinguish regular patients from heart failure patients in the Indonesian population. The study results are expected to be used in heart centers throughout rural areas in Indonesia, especially in peripheral regions, so that timely and accurate heart failure diagnosis becomes no more challenging.

METHODS

The research design is a cross-sectional diagnostic test using consecutive sampling. The target population in this study is echocardiography videos of clinically diagnosed chronic heart failure and normal patients

from the accredited echocardiography lab in Harapan Kita National Heart Center. This study was approved by the Harapan Kita National Heart Center Institutional Review Board. Echocardiographic examinations were carried out by a cardiologist or trained cardiovascular technicians using Vivid E9 echocardiography machines and M5Sc transducers. These data were analyzed in the workstation (EchoPAC PC; GE Vingmed Ultrasound US). Echocardiograms were obtained using apical 4-chamber (A4C), apical 2-chamber (A2C), and parasternal long-axis (PLAX). In assessing left ventricular structure and function, multiple features were extracted, including velocity, left ventricular end-systolic and end-diastolic volume and ejection fraction as calculated by Simpson's method⁸, the ratio between early mitral inflow velocity and mitral annular early diastolic velocity (E/e'), left atrial volume likewise left atrial volume index (LAVI) using biplane length method. The data was then saved in the cine-loop format for up to 5 heartbeat cycles with both left ventricles and left atrium clearly and wholly visualized. The frame rate of each image is 50 to 90 frames/second. Then, the results were validated by an expert echocardiologist based on national guidelines to reduce inter-observer variability.

Dataset Selection

The medical records for all inpatients and outpatients with chronic heart failure from January 2020 to October 2021 are obtained. Cardiologists established heart failure diagnoses based on clinical data, laboratory results, and echocardiography, which is the gold-standard method. Then, the authors screened data quality, completeness, and compatibility using our inclusion criteria. The inclusion criteria were echocardiographic data of patients with clinical presentation of shortness of breath and diagnosed as chronic heart failure by cardiologists. The echocardiography exam might be done during the patient's first encounter in clinic (non-emergency setting) or after multiple episodes of care/control. Exclusion criteria were: (1) arrhythmia, such as atrial fibrillation, (2) coexisting severe valvular heart disease, (3) incomplete echocardiography examination. The normal subjects included were completely health

population with no comorbidities, i.e., asthma or chronic obstructive pulmonary disease, with normal cardiac evaluation results. The minimum sample size is determined through the sample formula approach for diagnostic tests, where we find the minimum sample size to be 129 subjects, including a 10% possibility of dropouts.

Statistical Analysis

Statistical analysis was performed using RStudio program (version 2022.02.3+492.pro3, PBC, Boston). Numerical data are expressed as a mean or median with a standard deviation, while categorical data is presented in a percentage. Missing variables are assumed to be ‘missing at random (MAR) and handled using multiple imputations. The technique has yielded unbiased results for MAR even when there is a considerable proportion of missing data.¹⁰ Next, calibration, and discrimination are carried out. Calibration is an agreement between the reported and expected outputs, which in this study are HF/normal and HFrEF/HFpEF. The calibration was analyzed using the Hosmer-Lemeshow goodness-of-fit statistical test with $p > 0.05$, indicating that the score had a good calibration. Meanwhile, discrimination suggests the ability of ML to differentiate between HF and non-HF patients and is assessed using the ROC curve to obtain the AUC between the independent variable parameters and the dependent variable, then calculated the value of sensitivity, specificity, PPV, NPV, and LR.

Machine Learning Method

Our proposed method consists of two processes: pre-processing, where we prepare our data, and model training, where we train and evaluate our classification model. The overall flow of our proposed method is illustrated in **Figure 1**.

Pre-processing

We conducted several video pre-processing techniques to get the data ready for deep learning models. First, we perform cropping to get only the video’s center and eliminate the unnecessary pixel from each frame. Then, we resized each frame to be 128×128 in width and height, respectively. Then, we perform frame down-sampling to reduce the number of frames for each video. The number of frames to use is decided according to which video has the least frame. This has to be done since the input for the deep learning algorithm is fixed in dimension. Therefore, we resized each frame to a specific size and down-sampled the number of frames for each video to a particular number of frames. Lastly, each frame is normalized by dividing each pixel by 255, resulting in a value ranging from 0 to 1.

Model Training

We split the data into train and test using StratifiedKFold cross-validation with a K value of 5. VGG16 is used to help represent video into a sequence of vectors and then train a predominant deep learning algorithm for sequential problems,

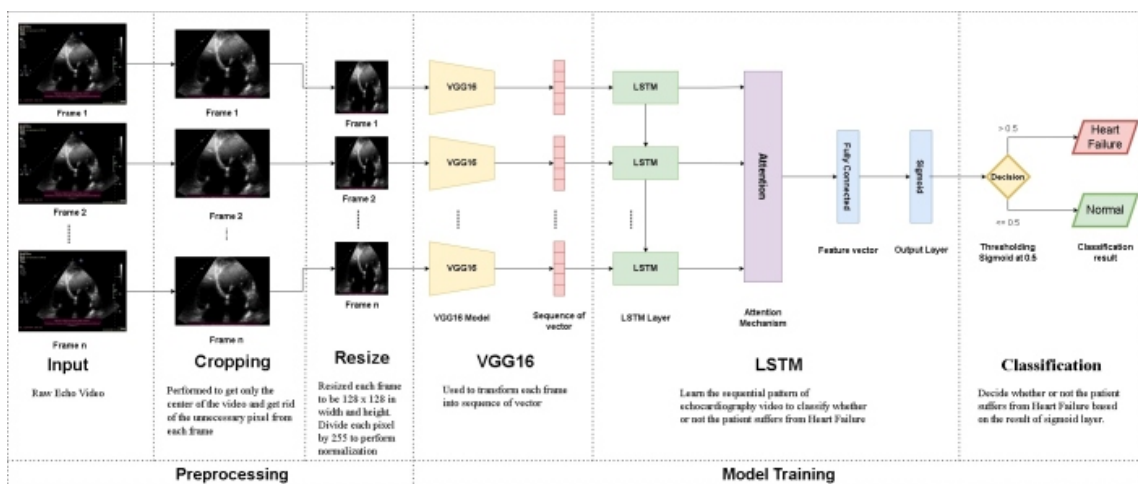


Figure 1. Illustration of the machine learning flow.

namely Long-Short Term Memory (LSTM).

VGG16 is a convolutional neural network (CNN) model developed by the Visual Geometry Group (VGG), University of Oxford¹³. VGG16 was trained on the Imagenet dataset and achieved state-of-the-art results in a well-known computer vision competition, Visual Recognition Challenge (ILSVRC), with an accuracy of 92,70%. VGG16 consists of 16 layers, as illustrated in **Figure 2**. Note that we only use VGG16 as an encoder to extract feature vectors out of each frame on which these feature vectors are then fed into LSTM to learn its sequential pattern; therefore, the weights and biases of VGG16 are frozen, and the softmax layer is removed.

Hochreiter first introduced LSTM to cover the limitation of recurrent neural network (RNN)

that suffers from vanishing gradient problems where the gradient cannot reach every layer. This problem occurs when the model is forced to learn a very long sequence. LSTM addressed this problem by introducing the so-called “Long Term Memory” (also known as cell state) denoted as C in **Figure 3**. This cell state does not go through any non-linear activation function; hence during the gradient descent, it is this cell state derivative that can prevent the LSTM gradients from vanishing. It has been shown that LSTM can learn long data sequences better than RNN.¹¹ A single cell of LSTM consists of several parts that are often called gates.

The first gate is called forget gate as highlighted in **Figure 4**. The forget gate is responsible to decide whether or not the model

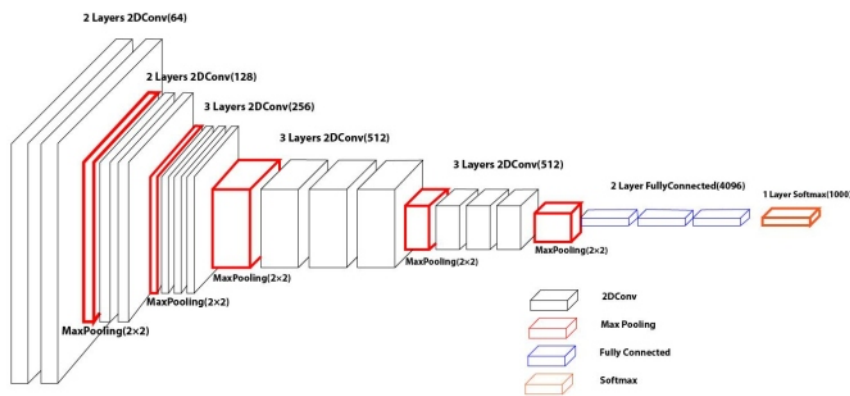


Figure 2. VGG16 architecture.

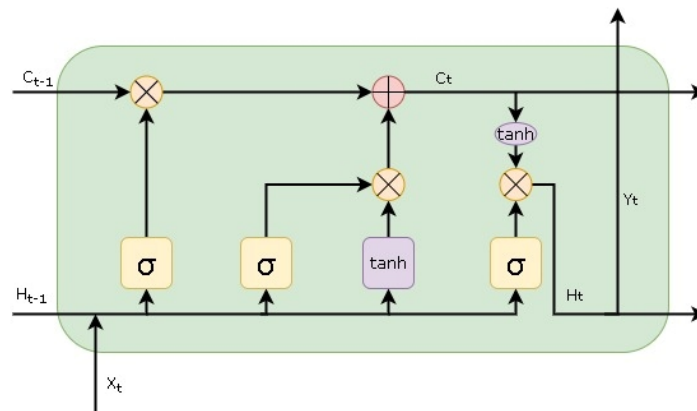


Figure 3. LSTM cell.

should keep the information from the previous timestamp. This gate uses a sigmoid activation function which produces output that's ranging from 0 to 1, this can be interpreted as how much the information from the previous timestamp is necessary for the model to remember.

The second gate is called the input gate as highlighted in **Figure 5**. The input gate is responsible to quantify the importance of the information from the current timestamp which the model will add this information to it's cell state. The input gate consists of two neurons, the first neuron (yellow rectangle) uses sigmoid activation function while the other (purple rectangle) uses tanh activation function. First, the new information along with the previous hidden state is being fed to the sigmoid neuron

resulting in a value ranging from 0 to 1. Then, the same thing is fed to the tanh neuron resulting in a value ranging from -1 to 1. On top of that, both the result of the sigmoid neuron and the tanh neuron are multiplied to decide how much information and whether to add or to subtract the new information to the cell state.

The last gate is called output gate as highlighted in **Figure 6**. The output gate is the final gate of the cell, it is responsible to calculate the new hidden state based on the new information, the previous hidden state, and the new cell state. Both this new hidden state and the new cell state are fed to the next timestamp if exist. The output of this output gate will be the final output of LSTM cell on the last timestamp denoted by Y_t in **Figure 6**.

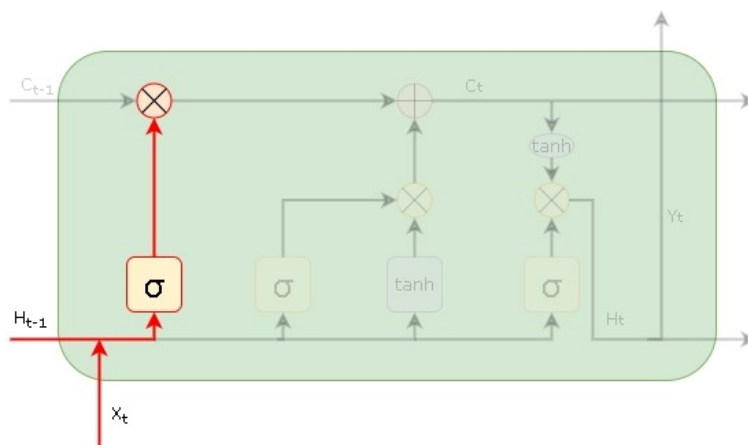


Figure 4. Forget gate.

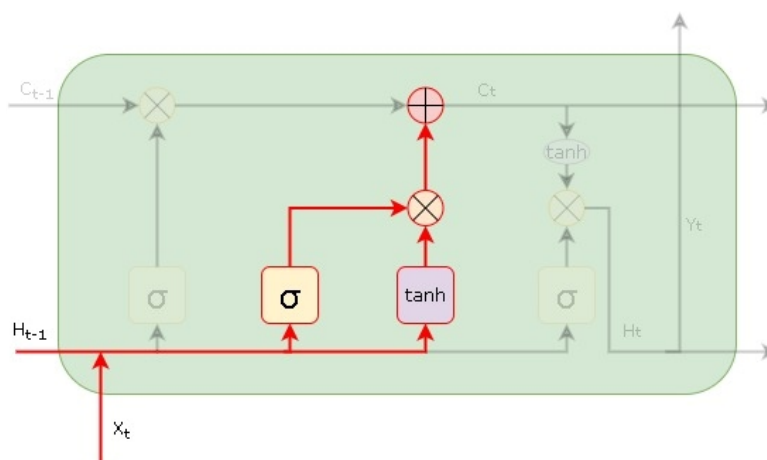


Figure 5. Input gate.

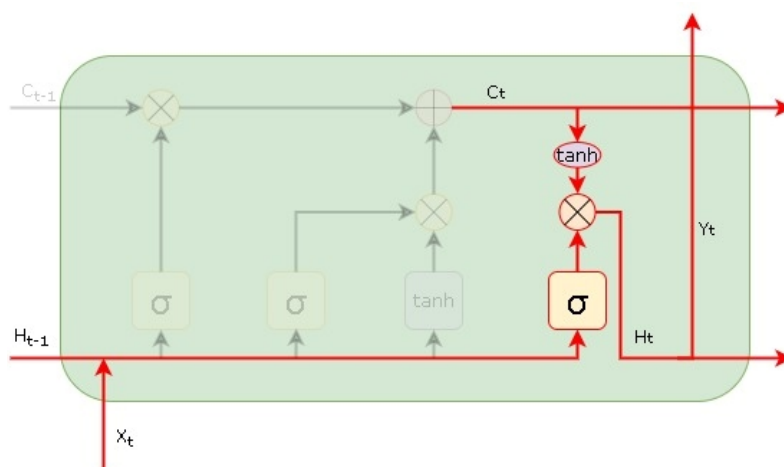


Figure 6. Output gate.

LSTM is exceptionally successful in many tasks such as handwriting recognition, speech recognition, machine translation, time-series classification, image captioning, video processing, etc.¹² We decided to use LSTM as we aim to capture the sequential pattern of a heart wall contraction in an echocardiography video with the hope that LSTM can make a reasonable prediction out of this pattern.

In addition, an attention layer is stacked on top of LSTM. When we provide a very long sequence of information, the models might ignore a few critical parts of the sequence, especially the starting part after processing the data. The attention mechanism helps the model memorize long sequences of information by taking the resulting calculation of LSTM at every timestamp. This mechanism also allows the model to pay more attention to which part of the sequence highly defines a specific class and weighs them more than others.

Lastly, the output layer consists of a sigmoid neuron. This layer is used to decide whether the patient suffers from heart failure by thresholding the output of the sigmoid neuron at 0.5, if the result of the sigmoid is greater than 0.5, then the patient is predicted to suffer from heart failure. Otherwise, the patient is predicted to be normal.

RESULTS

The characteristics of the subjects included in this study are given in **Table 1**. Male

represents 81,3% and 62.5% of normal and HF patients subjects, respectively. The median age is 36 in normal subjects, compared to 58 in HF patients, and both subject groups' median/mean of SBP and DBP are within the normal range. NTproBNP values were not obtained for normal patients as it was deemed unnecessary. The EF, E Peak Vel, A Peak Vel, E'med T0, and E'lat T0 in the HF group is lower compared to the normal group. On the other hand, the E/med e', E/lat e', E/ave e', LVEDV, LVESV, LA Volume and LAVI are higher than the normal category. The wall motion abnormality was also assessed during the echocardiographic examination. It turns out that 45 show global normokinetic, 21 with regional wall motion abnormality, 14 have apical akinetic, and 19 exhibit global hypokinetic.

We conducted a binary classification experiment to distinguish heart failure. The HFpEF and HFrEF classes are merged into one category, Heart Failure, while the normal category is left unchanged. In the end, it results in two types: Normal and Heart failure. The result of this experiment is shown in **Table 2**.

The sensitivity, and specificity of A2C for discriminating between HF and normal patients were 96.29% and 87.23%, respectively. Likewise, the highest accuracy was yielded by 92.96% in A2C and had the highest F1 score of 94.54%. The sensitivity and specificity of A4C were 96.34% and 80.43%, respectively, which yielded the highest sensitivity. Meanwhile, the

Table 1. Baseline study population characteristics.

Variables	Normal (N = 48)	Heart failure (N = 90)
Physical information		
Age, years	36 ± 9.65*	58 ± 12.78*
Gender, male	39/48 (81.3%)	55/88 (62.5%)
Systolic blood pressure, mmHg	125 ± 19.33*	120.3 ± 21.51***
Diastolic blood pressure, mmHg	75 ± 11.89*	70 ± 12.08*
Height, cm	166.6 ± 8.87***	160 ± 12.59*
Weight, kg	70.11 ± 15.59***	67 ± 15.52*
NTProBNP	N/A	1806 ± 15649.4*
Echocardiographic information		
EF (55-70)	68.40 ± 6.09***	47 ± 17.09*
E/A Ratio (0,75-1,5)	1.57 ± 0.37***	1.07 ± 1.01*
E Peak Vel (70-120)	85.36 ± 18.05***	79 ± 26.47*
A Peak Vel (42-70)	55.1 ± 17.98*	67.9 ± 31.64*
E'med T0 (>8)	10.65 ± 2.43***	4.9 ± 1.76*
E'lat T0 (>10)	13.30 ± 2.18*	7.18 ± 2.57*
E/med e' (<8)	7.9 ± 2.26*	16.11 ± 8.06*
E/lat e' (<8)	6.15 ± 1.59*	10.4 ± 5.31*
E/ave e' (<8)	7.00 ± 1.36*	13.3 ± 6.10*
LVEDV 64-85	101.0 ± 20.76*	132.0 ± 73.72*
LVESV 24-37	44.0 ± 9.78*	77.4 ± 67.41*
LA Volume (A4C) <28	38.00 ± 11.22*	60.9 ± 36.16*
LAVI A4C <28	21.10 ± 6.96*	36.8 ± 24.39*

*Median ± SD; **Proportion; ***Mean ± SD

Table 2. Test performance characteristics of the model.

View	Accuracy	F1	Precision	Sensitivity	Specificity	NPV	LR+	LR-
2 Chamber	92.96	94.54	92.85	96.29	87.23	93.18	7.54	0.0425
4 Chamber	90.62	92.94	89.77	96.34	80.43	92.50	4.92	0.0455
Plax	88.28	91.01	87.35	95.00	77.08	90.24	4.15	0.0649

PLAX-view gave sensitivity and specificity of 95% and 77.08%, respectively. The overall diagnostic accuracy of A2C, A4C, PLAX-view were 92.96%, 90.62% and 88.28%, respectively.

The models yielded good diagnostic performance for discriminating between HF and normal patients. The models had the best overall performance using the 2AC view, with a misclassification rate of 7.04%.

Figure 7 shows the receiver operating characteristic (ROC) curve of the resulting models where the more the line curved to the upper left, the better the model performance. The ROC curve could be quantified by calculating

the area under the curve (AUC), which we provided in the legend of the ROC figure. The random classifier indicated by the dashed red line assigns a score sampled from the uniform distribution between 0 and 1 to each instance. The rule of thumb is that no machine learning which roc curve should be under this red line. Our AUC values ranged from 0.84 (PLAX) to 0.93 (A2C). Furthermore, we performed significance testing between the test performance scores with a p-value threshold of 0.05, which we provided in **Table 3**. It can be inferred that there is no significant difference in terms of accuracy between each view compared to others.

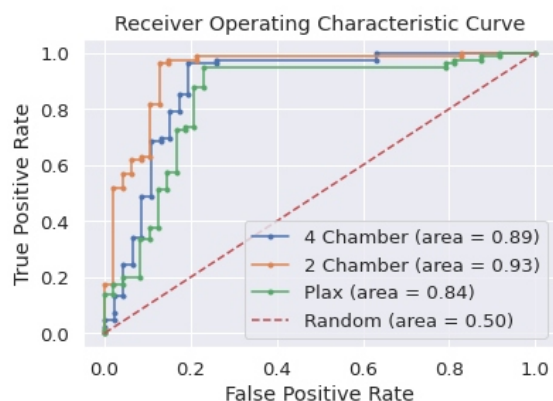


Figure 7. Receiver operating characteristic curve.

DISCUSSION

Cardiac emergencies necessitate a quick patient assessment, in addition to basic vital signs such as blood pressure, heart rate, and oxygen saturations, clinicians may need more information than vital signs. With echocardiography-ML, promptly collecting the echocardiographic helps reduce treatment options and discover plausible explanations for unstable vital signs in critically ill patients, especially in distant areas.

We provide a state-of-the-art comparison of machine-learning algorithms with human readers for diagnosing heart failure. On our findings, the mean age of the heart failure population was 58 ± 12.78 and male 62.5% (Table 1), which was also shown previously by Reyes and colleagues with a mean age of 57.8 and predominantly male (66%) in Indonesia.¹⁴

The model was tested using 128 echocardiograms and showed specificity levels ranging between 77% and 87%. The highest sensitivity levels above 96% were depicted in the A4C view. We found that our approach delivered accurate information with the area under the curve (AUC) above 0.84 using the echocardiography parameter. Similarly, a single-center study by Omar AM et al. (2017) involved 130 patients and showed a slight difference of AUC of 0.853 for estimating left ventricular diastolic dysfunction.^{15,17}

From our findings, the A4C view has the highest level of sensitivity compared to the other two views. A two-center study showed different results, which yielded accuracies of 97%, 97%, and 91% by using A2C, PLAX, and A4C views,

Table 3. The difference results in terms of accuracy between chamber and plax.

T-test	P-Value
2 Chamber / 4 Chamber	0.2381
2 Chamber / Plax	0.1356
4 Chamber / Plax	0.4334

respectively.⁸ The A4C view is one of the hardest to achieve accuracy. Apical views (A4C and A2C) also seem to suffer the most from lower resolution images. In A4C views, the program also captures the movement of the right ventricle, which can bias learning and make it difficult to detect the endocardial border, in contrast to 2CH and PLAX views which are more focused on one side.

The high sensitivity score of 4AC is mainly caused by the imbalanced class on which we train the model. Since we merged the HFpEF and HFrEF classes into a single category, namely HF, the class distribution turned out to be 1:2 for normal and HF. As a result, the model will make prediction attempts on the majority class more often than the minority class as the misclassification is mainly caused by the model mistaking normal for HF.

There are false positives and false negatives in our results. For this reason, we have carried out internal validation with several experts to match the misclassifications we found with clinical parameters. In our analysis, there are some discrepancies, such as an increase in the left atrial pressure with the normal ejection fraction, considered heart failure but detected by the machine as normal.

Interoperator variability during echocardiography and retrieval of several echocardiographic windows with an intermittent or absent endocardial border during analysis, such as lateral or anterior windows that disappear in the systole or diastole phase, could result in misclassification. Furthermore, the shifting of several windows between A2C and A4C can also influence the false positive and false negative rates in our study, where a subset of diagnosis has normal echocardiographic features but was read as heart failure and vice versa. Hence, this supports our hypothesis that using only one view

to differentiate between HF / normal through ML is possible.

According to Khamis, H. et al. (2017), there were several elements at play when working toward fully automatic heart functional assessment of echocardiograms and automatic classification of their standard views hence developing different values in each parameter.⁸ In addition to clutter, noise lowers the clarity of the images, thus limiting the ability to perform accurate view classification, (1) Physiological differences across participants, varying acquisition settings (angle, depth, scanning machine characteristics, foreshortening, etc.), and the sonographer's experience all contribute to intra-view variability of echocardiograms of the same cardiac view; (2) Identical information in both views (such as valve motion, wall motion, left ventricle, etc.), as well as poorly defined transducer location during collection, which may result in imprecise capture and confusing view, echocardiograms of various cardiac perspectives exhibit inter-view similarity; (3) Duplicated data, such as test details (examination date and time, ECG, heart rate, frame rate, and scanner details), which are present in all echocardiograms regardless of view, could taint the categorization procedure. Machine learning-based algorithms could reduce those shortfalls.⁹

The computational cost of our model is measured according to how much time it takes for the model to take the data from the input layer and gives the result on the output layer. We found that our model takes approximately $\pm 0.1489 - 0.1906$ seconds to predict a single sample of data. This prediction speed is also universally rapid, while normal examination would take around 15 to 60 minutes. Please note that this measurement does not include data acquisition from the pre-processing phase, and it ran on the following hardware:

- RAM 32 GB
- GPU: NVIDIA GeForce GTX 1080 Ti
- Processor: Intel (R) Core (TM) i7-6800K CPU @ 3.40GHz

Although there has been fully automated echocardiographic interpretation, which can automatically measure cardiac parameters

(ejection fraction, LV mass index, and left atrial volume index), which has been widely used to assist in diagnosis, our study provides a different approach using sequential pattern memory of echocardiographic.¹⁶ This tested machine learning algorithm proved fairly accurate and delivered relatively high sensitivity of echocardiogram videos compared to manual echocardiography calculation.

Additionally, as accurate interpretation of echocardiographic pictures may depend heavily on clinician expertise, performance performed by trained AI models may be superior to that of conventional, inexperienced doctors. Our approach, however, has the potential to be an effective prescreening tool for heart failure diagnosis because it is quick, accurate, and only reliant on 2AC, 4AC, and PLAX views. It also provides an automatic diagnostic workflow.

Study Limitation

This was a single-center study performed on patients with clinical indications for echocardiography. Even though the size of our test group can be considered negligible (128 patients) in the era of big data, the number of patients was sufficient to reach high levels of statistical significance compared with the reference technique. However, it is essential to note that this study may risk overfitting due to its small population. Extensive validation, preferably multi-center randomized controlled trials with a more significant number of patients, is required before they may be approved, reproducible, and generalizable for clinical use. In addition, combining multiple views to discriminate HF might help improve accuracy. Afterward, more studies to investigate the effect of clinical use of machine learning algorithms on patient outcomes. That being said, the prospect of high-performance computing may require significant financial investment and ethical clearance, yet it will reduce associated costs in the future.

Nevertheless, future studies with more significant numbers of patients and specific pathologies spanning a more comprehensive range of RV volumes and EF would be needed to confirm our findings further.

CONCLUSION

Method for automated categorization of HF and normal patients using a novel deep learning method called LIFES was presented. The proposed approach performs well in relation to manual echo by experts with high accuracy, sensitivity, and specificity rate. This study adds to the growing literature that ML-based algorithms can improve image interpretation efficiency and reliability and is the first of its kind to utilize LSTM to categorize HF and normal patients solely from echocardiography images. Further research is warranted to validate the method on a larger dataset and reduce bias. In the future, this method can be used in real-time in complete software that streams images directly from an ultrasound scanner. Hence, it can serve as a promising way to overcome challenges associated with current clinical workflow, streamline repetitive tasks, and provide preliminary interpretation in areas with insufficiently qualified cardiologists.

CONFLICT OF INTERESTS

The authors declare no competing interests and received no funding from any affiliations.

REFERENCES

1. Kaptoge S, Pennells L, De Bacquer D, et al. World health organization cardiovascular disease risk charts: Revised models to estimate risk in 21 global regions. *The Lancet global health*. 2019;7(10):e1332-e1345. [https://search.datacite.org/works/10.1016/s2214-109x\(19\)30318-3](https://search.datacite.org/works/10.1016/s2214-109x(19)30318-3). DOI: 10.1016/s2214-109x(19)30318-3.
2. Clerkin K, Fried J, Raikhelkar J, et al. COVID-19 and cardiovascular disease. *Circulation*. 2020;141(20):1648-55. <https://www.ncbi.nlm.nih.gov/pubmed/32200663>. DOI: 10.1161/CIRCULATIONAHA.120.046941.
3. Kusunose K, Haga A, Abe T, Sata M. Utilization of artificial intelligence in echocardiography. *Circulation J*. 2019;83(8):1623-9. https://www.jstage.jst.go.jp/article/circj/83/8/83_CJ-19-0420/_article/-char/en. DOI: 10.1253/circj.CJ-19-0420.
4. Dey D, Slomka PJ, Leeson P, et al. Artificial intelligence in cardiovascular imaging: JACC state-of-the-art review. *J Am Coll Cardiol*. 2019;73(11):1317-35. <https://www.ncbi.nlm.nih.gov/pubmed/30898208>. DOI: 10.1016/j.jacc.2018.12.054.
5. Raghavendra U, Acharya UR, Gudigar A, et al. Automated screening of congestive heart failure using variational mode decomposition and texture features extracted from ultrasound images. *Neural Comput Appl*. 2017;28(10):2869–78.
6. Sanchez-Martinez S, Duchateau N, Erdei T, et al. Machine learning analysis of left ventricular function to characterize heart failure with preserved ejection fraction. *Circ Cardiovasc Imaging*. 2018;11(4):e007138. DOI: 10.1161/CIRCIMAGING.117.0074
7. Kusunose K, Haga A, Abe T, Sata M. Utilization of artificial intelligence in echocardiography. *Circulation J*. 2019;83(8):1623-9. https://www.jstage.jst.go.jp/article/circj/83/8/83_CJ-19-0420/_article/-char/en. DOI: 10.1253/circj.CJ-19-0420.
8. Khamis H, Zurakhov G, Azar V, et al. Automatic apical view classification of echocardiograms using a discriminative learning dictionary. *Medical Image Analysis*. 2017;36:15-21. <https://doi.org/10.1016/j.media.2016.10.007>
9. Jiang Z, Lin Z, Davis L. 2013. Label consistent K-SVD: learning a discriminative dictionary for recognition. *Transactions on Pattern Analysis and Machine Intelligence*. 35:11.
10. Madley-Dowd P, Hughes R, Tilling K, Heron J. The proportion of missing data should not be used to guide decisions on multiple imputation. *Journal of Clinical Epidemiol*. 2019;110: 63–73. <https://doi.org/10.1016/j.jclinepi.2019.02.016>.
11. Goodfellow I, Bengio Y, Courville A. *Deep learning*. London, England: MIT Press; 2016.
12. Patterson J, Gibson A. *Deep learning a practitioner's approach*. Sebastopol, USA: O'Reilly Media; 2017.
13. Simonyan, Karen, Zisserman A. Very deep convolutional networks for large-scale image recognition. 3rd International Conference on Learning Representations, ICLR 2015 - Conference Track Proceedings. 2015. p. 1–14.
14. Reyes E, Ha J, Firdaus I, et al. Heart failure across Asia: Same healthcare burden but differences in organization of care. *Int J Cardiol*. 2016;233:163-7. <https://doi.org/10.1016/j.ijcard.2016.07.256>
15. Omar A, Narula S, Rahman M. et al. Precision phenotyping in heart Failure and pattern clustering of ultrasound data for the assessment of diastolic dysfunction. *J Am Coll Cardiol*. 2017;10:11. <https://doi.org/10.1016/j.jcmg.2016.10.012>.
16. Chiou Y, Hung C, Lin S. AI-assisted echocardiographic prescreening of heart failure with preserved ejection fraction on basis of intrabeat dynamics. *J Am Coll Cardiol*. 2021. <https://doi.org/10.1016/j.jcmg.2021.05.005>
17. Madani A, Arnaout R, Mofrad M, Arnaout R. Fast and accurate view classification of echocardiograms using deep learning. *Nature Partner Journals*. 2018;1:6. doi:10.1038/s41746-017-0013-1.